A hadronic calorimeter based on resistive micropattern gaseous detectors

L. Generoso(1)(2), M. Ali(1)(7), M. G. Alviggi(3), M. Bianco(6), M. Borysova(4), M. Biglietti(5), M. Buonsante(1)(2), M. T. Camerlingo(1), A. Colaleo(1)(2), M. Della Pietra(3), R. Di Nardo(5), K. Flöthner(6), P. Iengo(3), M. Iodice(5), L. Longo(1), M. Maggi(1), L. Moleri(1), F. Nenna(1)(7), E. Oliveri(6), A. Pellecchia(1)(2), R. Radogna(1)(2), L. Scharenberg(6), G. Sekhniaidze(3), F. M. Simone(1)(2), A. Stamerra(1)(2), P. Verwilligen(1), R. Venditti(1)(2), D. Zavazieva(4), and A. Zaza(1)(2)

(1) *INFN - Sezione di Bari, Via Amendola 173, Bari, Italy*
(2) *Università degli studi di Bari Aldo Moro, Piazza Umberto I, Bari, Italy*
(3) *INFN - Sezione di Napoli, Via Cintia, Napoli, Italy*
(4) *Weizmann Institute of Science, Herzl St 234, Rehovot, Israel*
(5) *INFN - Sezione di Roma 3, Via della Vasca Navale, 84, Roma, Italy*
(6) *CERN, Esplanade des Particules 1, Meyrin, Switzerland*
(7) *Università degli Studi di Padova, Via VIII Febbraio, 2, Padova, Italy*

Summary. — Precise energy measurements will be crucial at future Higgs factories to reliably identify hadronic decays of W, Z, and Higgs bosons. Achieving this requires the use of the Particle Flow Algorithm (PFA), which relies on calorimeters with fine-granularity readouts. In response, a novel hadronic calorimeter (HCAL) has been designed using resistive Micro Pattern Gaseous Detectors (MPGDs) as active medium. MPGDs combine excellent spatial and timing resolution, radiation hardness, and fine-granularity readouts, making them well-suited for next-generation collider experiments, optimized for PFA. This contribution reports on performance studies of MPGD prototypes at CERN SPS, focusing on efficiency and time resolution, along with energy response measurements of an HCAL cell prototype tested with pion beams at CERN PS.

1. – MPGD-based readout for calorimetry at future colliders

Among the primary objectives of the next-generation colliders is the achievement of a jet energy resolution of less than 3-4% at 100 GeV for effective Z/H separation, attainable through a Particle Flow approach [1]. This relies on high-granularity calorimetry capable of resolving individual jet constituents, thereby enhancing the matching between tracker and calorimeter, and ensuring that each particle energy is measured by the best-performing detector subsystem. A second key goal is the implementation of five-dimensional calorimetry, which integrates both spatial and timing information of energy deposits to improve shower reconstruction and enhance background rejection.

To meet both objectives, current R&D efforts are directed toward the development of a sampling hadronic calorimeter (HCAL) that combines iron absorbers with resistive Micro Pattern Gaseous Detectors (MPGDs) as active elements. This design not only features a fine spatial granularity of 1 cm^2 but also ensures high radiation hardness, withstanding doses of several C/cm^2 [2], while maintaining cost-effectiveness for large-scale applications. Furthermore, resistive MPGDs provide excellent time resolution at the nanosecond level [3, 4], high-rate capabilities [5], operational stability due to discharge quenching, and good uniformity, making them ideal for calorimetry. The performance of this MPGD-based HCAL is currently being investigated through dedicated simulations in the framework of the Muon Collider [6, 7, 8]. Modeled as a 60-layer sampling calorimeter with 3 mm argon gaps and 22 mm iron absorbers, the detector demonstrates an energy resolution of $45\%/\sqrt{E} \oplus 12\%$ with semi-digital readout, approaching the performance targets for next-generation calorimetry. In parallel, the hardware development of the HCAL cell prototype is progressing through test beam campaigns, exploring various technologies such as resistive MicroMegas [9], μ-RWELLs [10], and RPWELLs [11].

2. – Characterization of an MPGD-HCAL cell prototype

Several resistive MPGD technologies are being investigated to determine their suitability for calorimetry readout through dedicated beam tests. The tested prototypes include 7 μ-RWELLs, 4 resistive MicroMegas, and 1 RPWELL. All twelve devices have an active area of 20×20 cm^2, a drift gap with a thickness of 6 mm, and a readout board consisting of 384 pads, each measuring $1\times1 cm^2$. Their performance was studied using muon beams with energies around 100 GeV at the CERN SPS. Additionally, an MPGD-HCAL cell prototype, incorporating stainless steel absorbers, was characterized with pion beams in the 1 to 10 GeV energy range at the CERN PS.

2˙1. *Detector performance with MIPs.* – Detector efficiency and response uniformity were evaluated using minimum ionizing muons with energies around 100 GeV, during test beam campaigns at the CERN SPS in 2023 and 2024. All twelve MPGD prototypes were operated with argon-based gas mixtures: the μ-RWELLs used $Ar:CO_2:CF_4$ in a 45:15:40 ratio, while the MicroMegas and RPWELL employed $Ar:CO_2$:iC4H10 in a 93:5:2 mixture. Signal readout was performed using APV25 front-end electronics [12], interfaced with the RD51 scalable readout system (SRS) [13].

Detector efficiency was assessed using reconstructed muon tracks from an external tracking system as a reference. All technologies reached efficiency plateaus consistent with their geometrical acceptance: MicroMegas and the RPWELL achieved up to 95%,while μ-RWELLs approximately 75%. In particular for the μ-RWELLs, the efficiency is constrained by the dead areas related to the charge evacuation lines (PEPs) [10].

For response uniformity - defined as the ratio of the standard deviation to the mean of the charge distribution in track-matched clusters - MicroMegas demonstrated the most stable behavior with a variation of about 10%, followed by μ-RWELLs at 16% and RPWELL at 23%. Some localized non-uniformities were observed in the μ-RWELLs, requiring further dedicated studies [6].

2˙2. *Efficiency studies for μRWELLs*. – Current efforts are focused on integrating fast, high-rate electronics with MPGD prototypes. As part of this, a test beam campaign in September 2024 evaluated the performance of a μ-RWELL detector read out with VMM3a-based front-end electronics [14], using muon beams of approximately 100 GeV. The VMM3a chip enables operation at low analog thresholds (down to 0.8 fC) and high rates on the order of MHz/cm^2.

The detector was operated within a beam telescope setup, consisting of three triple-GEM tracking detectors and three plastic scintillators for triggering, all instrumented with VMM3a chips and read out via the RD51 scalable readout system (SRS). Detector performance was characterized by scanning a broad range of drift and amplification fields, as well as varying analog thresholds. Two argon-based gas mixtures were tested: Ar:CO_2:CF_4 (45:15:40) and Ar:CO_2 (70:30).

Efficiency was estimated using clusters matched to tracks reconstructed by the telescope. As shown in Figure 1 on the left, the charge MPV peaked at a drift field of 2.5-3 kV/cm, largely independent of the amplification voltage, consistently with X-ray gain studies [15]. While charge collection decreases at higher drift fields, the overall efficiency improves for amplification voltages above 520 V, as shown in Figure 1 on the right.

The efficiency map in Figure 2 shows localized dips near the PEPs. These dips become narrower and shallower with increasing drift field, enhancing charge collection in those regions and improving global efficiency. This behavior is also observed in data collected with APV electronics and thus is independent of the readout chip.

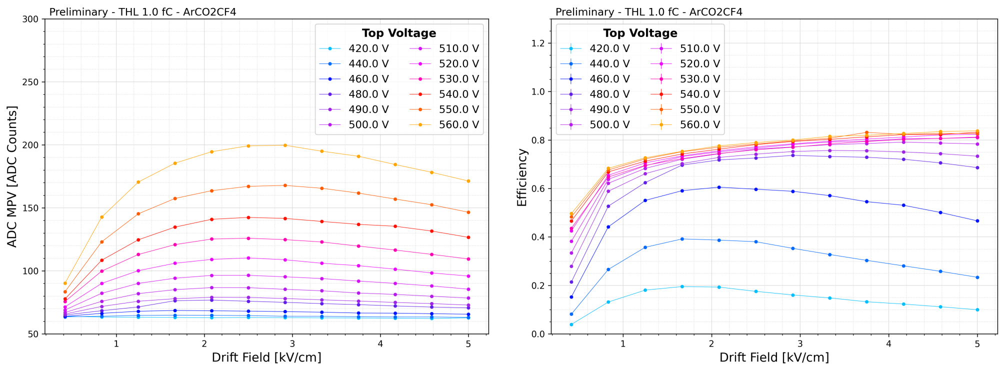

Fig. 1. – *Left*: μ-RWELL most probable value (MPV) of the Landau fit to the charge distributions as a function of the drift field. *Right*: μ-RWELL efficiency as a function of the drift field. Data are taken in Ar:CO_2:CF_4 and with an analog threshold of 1 fC. Different colors represent different values of the amplification voltage .

The comparison between the gas mixtures reveals that the Ar:CO_2 mixtures allow for higher charge multiplication than Ar:CO_2:CF_4, leading to an extended gain range, as shown on the left of Figure 3. At low charge values (below 100 ADC), the turn-on curves for both mixtures overlap, indicating similar initial response characteristics. However, as the charge increases, a slightly higher efficiency plateau (a few percentage points) is observed for Ar:CO_2 gas mixture.

Studies on the time resolution of the μ-RWELL have been carried out using muon tracks reconstructed in the tracker as a temporal reference t_{track}. The time of the cluster in the μ-RWELL t_{cluster} corresponds to the peaking time of the signal measured by

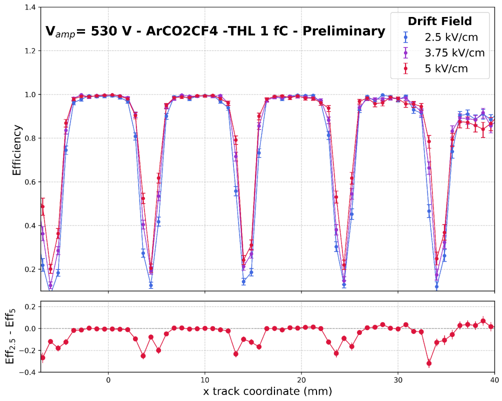

Fig. 2. – *Upper:* μ-RWELL efficiency integrated along the PEP line direction as a function of the orthogonal direction (x track coordinate) in Ar:CO_2:CF_4 and with an analog threshold of 1 fC and an amplification voltage of 530 V. Different colors represent different values of the drift field. *Lower:* Efficiency differences between drift fields of 5 kV/cm and 2.5 kV/cm.

the VMM3a electronics. The distributions of the time difference between the t_{track} and t_{cluster} are fitted with a Gaussian, whose sigma represents the measured time resolution. The latter accounts for both the time resolution of the μ-RWELL and the uncertainty of the track. To asses the intrinsic time resolution of the detector under test, the known tracking time resolution is subtracted in quadrature to the σ_{meas}, yielding the results shown on the right of Figure 3. The best time resolution achieved was approximately 6 ns, obtained with an Ar:CO_2:CF_4 (45:15:40) gas mixture at an amplification voltage of 560 V and a drift field around 4.5 kV/cm. Finally, the results observed for the detector read out by the VMM3a chip are consistent with those obtained using the APV25, when operated at the same working point in terms of amplification, drift field, and analog threshold.

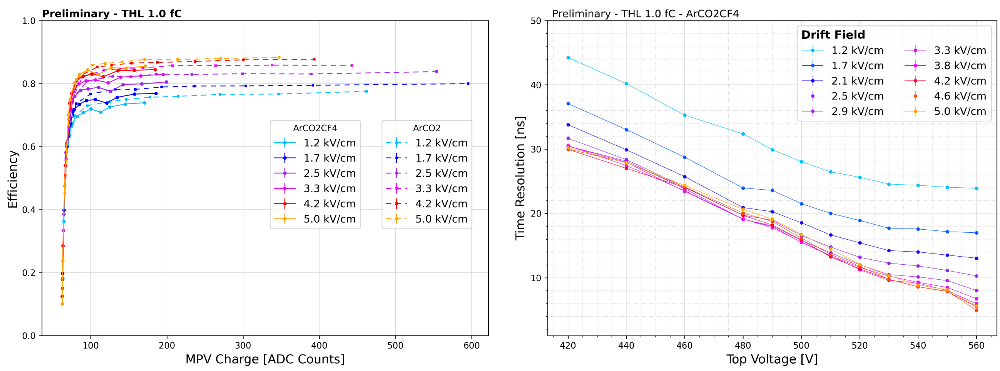

Fig. 3. – *Left:* μ-RWELL efficiency as a function of the charge MPV in Ar:CO_2:CF_4 (solid lines) and Ar:CO_2 (dashed lines). *Right:* μ-RWELL time resolution in Ar:CO_2:CF_4 as a function of the amplification voltage. Data are taken with an analog threshold of 1 fC. Different colors represent different values of the drift field.

2˙3. *Study of pion showers*. – A prototype calorimeter cell has been constructed by alternating eight layers of steel absorbers with eight MPGD detectors, each with an active area of 20×20 cm^2. The first two absorber layers have a thickness of 4 cm, while the following layers are 2 cm thick. The prototype was designed to anticipate the start of the shower, resulting in a total length of one nuclear interaction length (λ_I). The development of hadron showers was studied using negative pion beams in the energy range of 1–9 GeV at CERN PS in 2023 and 2024. The data were analyzed through a digital readout approach, counting the total hits above a given threshold for each event. MIP events, identified by having at most one hit per layer, were discarded from the analysis. The plot in Figure 4 shows good linearity between the nominal energy of the pion beam and the total number of hist in the HCAL prototype.

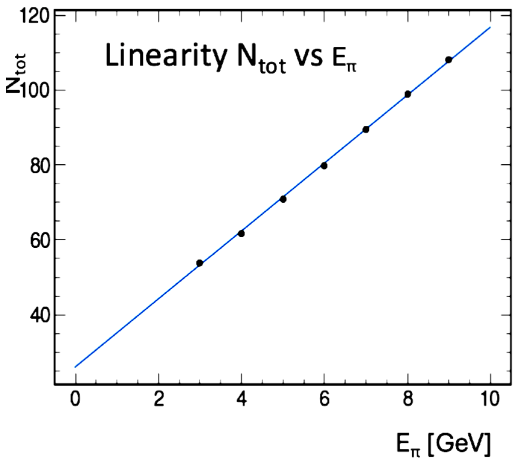

Fig. 4. – Total number of hits above the read-out threshold in the HCAL prototype as a function of the nominal energy of the pion beam at CERN PS.

3. – Conclusions and Outlook

The proposed MPGD-based HCAL represents an innovative and promising calorimeter design, particularly well-suited for Particle Flow reconstruction in future circular collider experiments, owing to its fine granularity (1cm^2) and good intrinsic energy resolution. The MPGD candidate technologies tested so far have demonstrated good overall gain uniformity, though further studies are ongoing to investigate the response patterns in some μ-RWELLs. The detector efficiencies are excellent and mostly limited by structural elements, with 95% plateaus for MicroMegas and the RPWELL, and ∼85% for μ-RWELLs. For μ-RWELLs, an increase in the drift field allows for a partial recovery of the efficiency drop observed close to the evacuation lines. New μ-RWELL prototype designs will incorporate a novel PEP-DOT DLC grounding [10], which will significantly increase acceptance and, consequently, overall efficiency. The 1 λ_I HCAL cell prototype has shown good linearity in the number of hits as a function of the beam energy when using a digital readout approach. Further optimization of energy resolution through a semi-digital method is under investigation. Moving forward, four large detectors with 121 mm^2 pads, covering an active area of 50×50 cm^2, will be produced and tested. These chambers will be integrated into the HCAL cell prototype alongside extractable iron absorbers, extending the current setup into a 2 λ_I calorimeter. Additional studies will aim to fine-tune the drift gap width of the MPGD chambers, optimize the gas mixture to enhance timing performances, and integrate fast, high-rate readout electronics in addition to VMM3a. Finally, this R&D effort will culminate in a joint test beam campaign with the ECAL CRILIN project [16], foreseen for 2026.

* * *

The author acknowledges the support under the National Recovery and Resilience Plan (NRRP), Mission 4, Component 2, Investment 1.1, Call for tender No. 104 published on 2.2.2022 by the Italian Ministry of University and Research (MUR), funded by the European Union – NextGenerationEU– Project Title: CALORHINO – CUP 53D23000990006-CALORHINO - Grant Assignment Decree No. 974 adopted on 30/06/2023 by the Italian Ministry of Ministry of University and Research (MUR)

REFERENCES

[1] Thomson M.A., *Particle flow calorimetry and the PandoraPFA algorithm*, *Nucl. Instrum. Methods Phys. Res. A*, **611** (2009) 25–40.
[2] Farina E. and al., *Resistive Micromegas high-rate and long-term ageing studies at the CERN Gamma Irradiation Facility*, *Nucl. Instrum. Methods Phys. Res. A*, **1042** (2022) 167423.
[3] Morello G. and al., *Advances on micro-RWELL gaseous detector*, *PoS*, **BORMIO2017** (2017) 002.
[4] Iodice M. and al., *Towards large size pixelized Micromegas for operation beyond 1 MHz/cm*^{2}, *JINST*, **18** (2023) C06029.
[5] Camerlingo M.T. and al., *Rate capability and stability studies on small-Pad resistive Micromegas*, *PoS*, **ICHEP2020** (2021) 825.
[6] Longo L. and al., *MPGD-based Hadronic calorimeter for a future experiment at Muon Collider*, *PoS*, **ICHEP2024** (2024) 1082.
[7] Accettura C. and al., *Towards a muon collider*, *Eur. Phys. J. C*, **83** (2023) 864.
[8] MuonColliderSoft, *MuonColliderSoft: Software repository for muon collider studies*, `https://github.com/MuonColliderSoft`.
[9] Iodice M. and al., *Small-pad Resistive Micromegas: Comparison of patterned embedded resistors and DLC based spark protection systems*, *J. Phys. Conf. Ser.*, **1498** (2020) 012028.
[10] Bencivenni G. and al., *The μ-RWELL for future HEP challenges*, *Nucl. Instrum. Methods Phys. Res. A*, **1069** (2024) 169725.
[11] Zavazieva D. and al., *Towards a large-area RPWELL detector: design optimization and performance*, *JINST*, **18** (2023) P08009.
[12] French M.J. and al., *Design and results from the APV25, a deep sub-micron CMOS front-end chip for the CMS tracker*, *Nucl. Instrum. Methods Phys. Res. A*, **466** (2001) 359–365.
[13] Martoiu S. and al., *Development of the scalable readout system for micro-pattern gas detectors and other applications*, *JINST*, **8** (2013) C03015.
[14] Pfeiffer D. and al., *Rate-capability of the VMM3a front-end in the RD51 Scalable Readout System*, *Nucl. Instrum. Methods Phys. Res. A*, **1069** (2022) 166548.
[15] Bencivenni G. and al., *The micro-Resistive WELL detector: a compact spark-protected single amplification-stage MPGD*, *JINST*, **10** (2015) P02008.
[16] Ceravolo S. and al., *Crilin: A CRystal calorImeter with Longitudinal InformatioN for a future Muon Collider*, *JINST*, **17** (2022) P09033.